TRIBOLOGIA - Finnish Journal of Tribology 3-4 vol 42/2025

https://doi.org/10.30678/fjt.160984

SUOMEN TRIBOLOGIAYHDISTYS RY
THE FINNISH SOCIETY FOR TRIBOLOGY
www.tribologysociety.fi
https://journal.fi/tribologia

A comprehensive evaluation of the abrasive wear mechanism of A356 / (0&5) wt.% SiCp Metal Matrix Composite in unidirectional and reciprocating contacts

Biju P. V.[1, 3, 4], Manesh K. K.[1, 3], V. R. Rajeev[2, 3]
[1]Government Engineering College, Thrissur, Kerala, India - 680009
[2]College of Engineering Trivandrum, Kerala, India - 695016
[3]APJ Abdul Kalam Technological University, Govt. of Kerala, India - 695017
[4]Vidya Academy of Science and Technology, Thrissur, Kerala, India - 680501
Corresponding author: Biju P. V.

ABSTRACT

The abrasive wear behaviour of A356 aluminium alloy and A356/5 wt.% SiCp composites were examined under unidirectional (USM) and reciprocating sliding modes (RSM) against 800 grit SiC abrasive medium. Wear maps developed at varying loads and velocities over a 25 metre sliding distance revealed that severe wear initiates at lower loads in RSM than USM, particularly in the base alloy. The composite exhibited enhanced wear resistance with a delayed onset of severe wear. Stereo microscopy and SEM analyses showed that RSM results in deeper, wider grooves and more surface degradation. Groove width in RSM was nearly three times greater than in USM, indicating increased wear severity. EDAX analysis revealed higher oxygen content in USM, suggesting the formation of an oxide layer which contributed to reduced friction. Overall, the findings highlight the critical role of sliding mode and SiCp (Silicon Carbide Particulates) reinforcement in influencing wear mechanisms and surface integrity in A356-based materials.

Keywords: A356 Alloy, A356/5 wt.% SiC_p composite, Unidirectional and reciprocating contacts, Abrasive wear maps, Wear mechanism, SEM & EDAX analysis

1. Introduction

Aluminium alloy-based metal matrix composites (AMMCs), reinforced with hard ceramic particles, exhibit superior wear resistance, making them ideal for tribological applications such as rotating impellers and paddles in abrasive slurry environments. Their enhanced performance is attributed to high hardness and fracture toughness, which reduce wear compared to conventional materials [1]. High-volume fractions of reinforcement particles improve wear resistance by lowering the real contact area and reducing temperature rise and friction. Studies (e.g., X.Y. Li et al.)[2] confirm this enhanced performance, especially under abrasive conditions. Empirical analyses by Mondal and S. Das [3] highlight the impact of load, abrasive size, and microstructural factors on wear behaviour. Larger particles tend to fracture and detach under stress, reducing overall wear resistance. Wear per unit sliding distance increases linearly with applied load but is relatively insensitive to abrasive size, with notable transitions occurring at critical abrasive sizes [4,5].

Effect of load and reciprocating velocity on the transition from mild to severe wear behavior of Al–Si–SiCp composites in reciprocating conditions have done by V R Rajeev et al. [6] and despite extensive research, limited studies focus on reciprocating abrasivewear conditions. Odabaş et al. [7] found higher wear losses under unidirectional wear at low velocities. X.Y. Li et al. also examined the formation of mechanically mixed layers during sliding, linking wear layer composition to load intensity.

Real-world applications, such as piston–cylinder systems in marine engines, illustrate the severe effects of reciprocating three-body abrasive wear. Entrapped debris intensifies the wear process, highlighting the need for more targeted research. To address this, the current study employs a patented reciprocating wear test rig with 18.3 µm abrasive particles, exploring higher velocities and stroke lengths than previous research [8,9,10]. This investigation compares unidirectional and reciprocating sliding wear modes under identical conditions to better understand how motion profiles affect AMMC performance. The findings offer insights into reinforcement strategies and material selection, supporting enhanced wear resistance and durability in sectors like automotive, aerospace, mining, and defence.

2. Materials and methods

2.1 Composite material preparation

A356 alloy and its 5 wt.% SiCp reinforced composite were produced using the liquid metallurgy stir casting route (LMSCR). The alloy was derived from Al 6061 in a diesel-fired tilting furnace with Al-50% Si and Al-50% Cu

Table 1. Chemical composition of A356 alloy

Element	Al	Si	Cu	Mg	Fe	Zn	Others
Wt.%	90-93	6-7.5	0.25	0.45	0.6	0.35	Balance

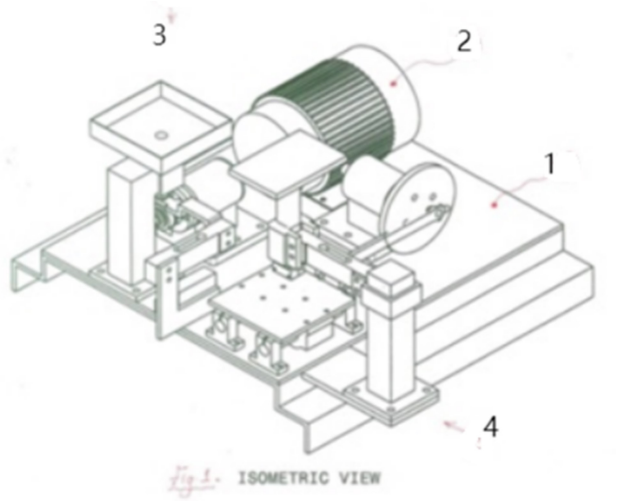

Figure 1. Illustrates the isometric view of in-house designed and developed pin-on reciprocating plate abrasive wear and coefficient of frictions test rig [Patent grant No. 414730, dated 16/12/2022.] 1.Base structure 2. Electric motor 3. Rotary Module 4. Reciprocating Module

master alloys. A356/5 wt.% SiCp composites were fabricated by stir casting [11]. Chemical composition of A356 Alloy is shown in Table 1.

Silicon carbide particles SiCp, 32 µm sourced from Carborundum Ltd., Cochin, were cleaned with distilled water for three days and dried. In the stir casting process [12], A356 ingots were melted in an electric furnace at 750 ° C, then stabilised at 650 °C. After slag removal, stirring was performed at 350 rpm while preheated SiCp (450°C for 4 hours) was added using a hopper. Prior to this, 1 wt.% Mg [13] was added to improve wettability. The composite melt was then cast into a metallic die for solidification.

2.2 Methods

For microscopic and hardness evaluation, the samples of required sizes of 10 x10 x10 mm^3 were cut from the as cast A356 and A356/5 wt.% SiCp composite using wire cut EDM (Electrical Discharge Machining). Also for abrasive wear study, test pins of sizes 6mm diameter and 32 mm length were prepared. The entire test samples were heat treated to T6 condition which involved solutionizing the samples at 530–550 °C for a prescribed duration to facilitate the dissolution of Mg_2Si and other soluble phases into the aluminium matrix. Following solution treatment, the specimens were quenched in water at ambient temperature to retain the alloying elements in a supersaturated solid-solution state. Subsequently, the quenched samples underwent artificial ageing at 150–180 °C for 4–8 h, during which controlled precipitation of fine Mg_2Si particles occurred.[14]

2.2.1 Microstructure analysis and Hardness measurement

Micrograph of A356 alloy and 5 wt.% SiCp composites were obtained using a Leica DM2700M optical microscope (Germany). Samples were metallographically polished and made parallel before Brinell hardness testing, performed with a 5 kgf load for 5 seconds using a Brinell hardness ball indenter. The average of three readings was reported.

2.2.2 Abrasive wear test in Reciprocating Sliding Mode and unidirectional sliding mode

Two-body abrasion tests were conducted using a custom-built pin-on-plate reciprocating tribometer. Three runs were performed to obtain average wear loss. The setup includes a reciprocating EN31 hardened steel plate fitted with 800-grit SiC abrasive paper. Figures 1 shows the test rig with 100 mm stroke length.

Table 2 provides the details of unidirectional and reciprocating abrasive wear test parametric conditions

Table 2. Details of experimentation

Parametric configurations at different test conditions						
Test conditions	Load (N)	Sliding Velocity (m/s)	Sliding distance (m)	Wear track (mm)	Abrasive medium	Sliding distance per cycle (mm)
Pin-on- rotating disc	5-12.5	0.2-0.8	25	31.85 (Radius)	18.3 microns SiC	200
Pin-on-reciprocating plate	5-12.5	0.2-0.8	25	100 mm (Stroke)	18.3 microns SiC	200

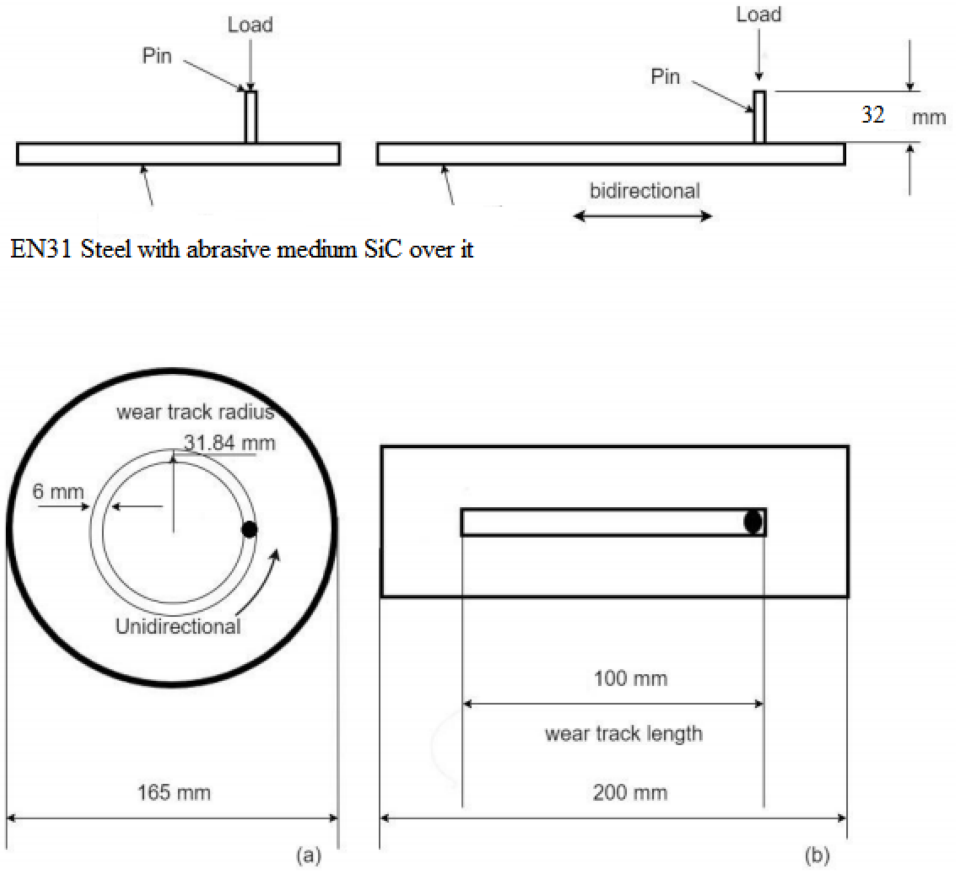

Figure 2. Schematic diagram showing A356–(0-5) wt.% SiC_p composite/ abrasive medium of grit size 18.3 microns placed on EN31 steel tribo-pairs tested under (a) unidirectional (wear track radius 31.84 mm) and (b) reciprocating (wear track length 100 mm) dry sliding conditions, with total sliding distance 200 mm per cycle for both the tribo-pairs.

followed for the study. Fig. 2: shows a schematic diagram showing A356–(0-5) wt.% SiCp composite/ abrasive medium of grit size 18.3 microns placed on EN31 steel tribo-pairs tested under (a) unidirectional (wear track radius 31.84 mm) and (b) reciprocating (wear track length 100 mm) dry sliding conditions, with total sliding distance 200 mm per cycle for both the tribo-pairs.

To compare abrasive wear behaviour of A356 alloy and its SiCp reinforced composite in reciprocating and unidirectional modes, tests were also conducted using a pin-on-disc rig (Model: TR20-LE, DUCOM, Bangalore).

Tests were performed across loads of 5–12.5 N, velocities of 0.2–0.8 m/s, and a 25 m skid length. Each test used fresh 800-grit SiC abrasive paper (After a certain minmum duration corresponding to load, new abraisve medium was used) ensuring full contact with the specimen surface. The contact between the pin and the sand paper is uniform and not concentrated on the some edge by ensuring/checking the flatness of the surface on which abrasive medium is fixed using spirit level during some interval of experimentation. Weight loss was determined using a 0.01mg. accuracy balance after cleaning with acetone and drying. Frictional force was measured using calibrated strain gauges, and the coefficient of friction (CoF) was calculated.

$$\text{Coefficient of friction} = \frac{\text{Frictional force}}{\text{Normal force}} \quad (1)$$

SEM/EDAX analysis was done using scanning electron microscopy of Make: Philips and Model: XL-30.

3. Results & Discussion

3.1 Microstructure and Hardness

Figure 3 shows the optical micrograph of (a) A356 alloy and (b) A356/5wt.% SiCp composite (T6 condition). Microstructure images were taken using an optical microscope (Leica DM2700M, Germany) of the sample cut from the T6 heat treated stir cast composite specimen. Figure 3(a) showed the presence of micro structure features such as α aluminum and eutectic silicon in A356 alloy. Figure 3(b) also showed that SiCp were uniformly distributed and the prepared A356/5 wt.% SiCp composites was having good bonding characteristics between SiCp and matrix. Further the T6 heat treatment of the alloy and its composite enhanced the hardness from 72 BHN to 82 BHN (with standard errorbars) due to the formation of inter metallic compounds such as Mg_2Si and Cu Al_2 during precipitation hardening.

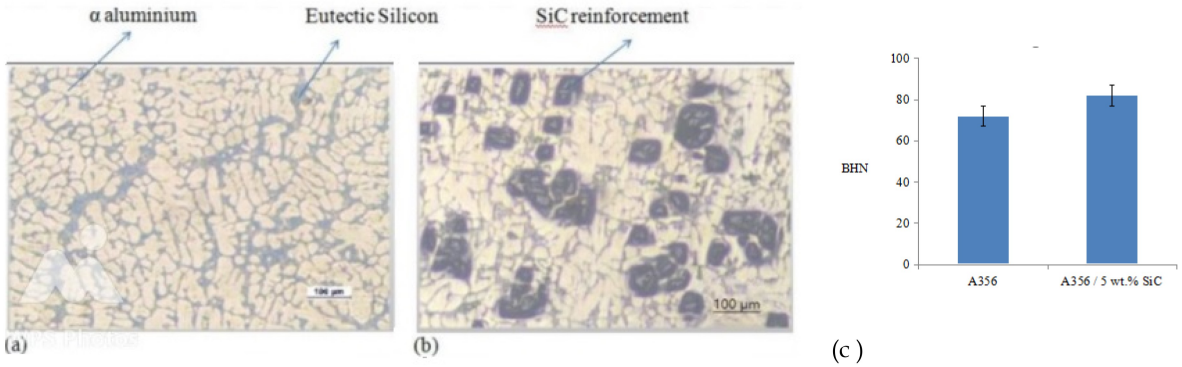

Figure 3. Optical micro graph of (a) A356 alloy and (b) A356/5wt.% SiC_p composite (T6 condition) (c) Variation of Brinell Hardness values in A356 alloy and A356/5wt.% SiC_p composite

3.2 Abrasive Wear map and CoF variation of A356 alloy & A356/5 wt.% SiCp composite in unidirectional and reciprocating contacts

Figure 4 depicts the wear mechanism maps (A, T. Alpas and J.D, Embury ,1991)[16] for different load and velocity conditions for a) A356 alloy in USM b) A356 alloy in RSM c) A356+5wt.% SiCp composites in USM d) A356+5wt.% SiCp composites in RSM against 800 grit SiC abrasive medium for a sliding distance of 25 metre. Abrasive wear rate is calculated by dividing the wear loss by the sliding distance. Values multiplied by 10^{-5} indicate the wear rate. (Severe abrasive wear means higher wear

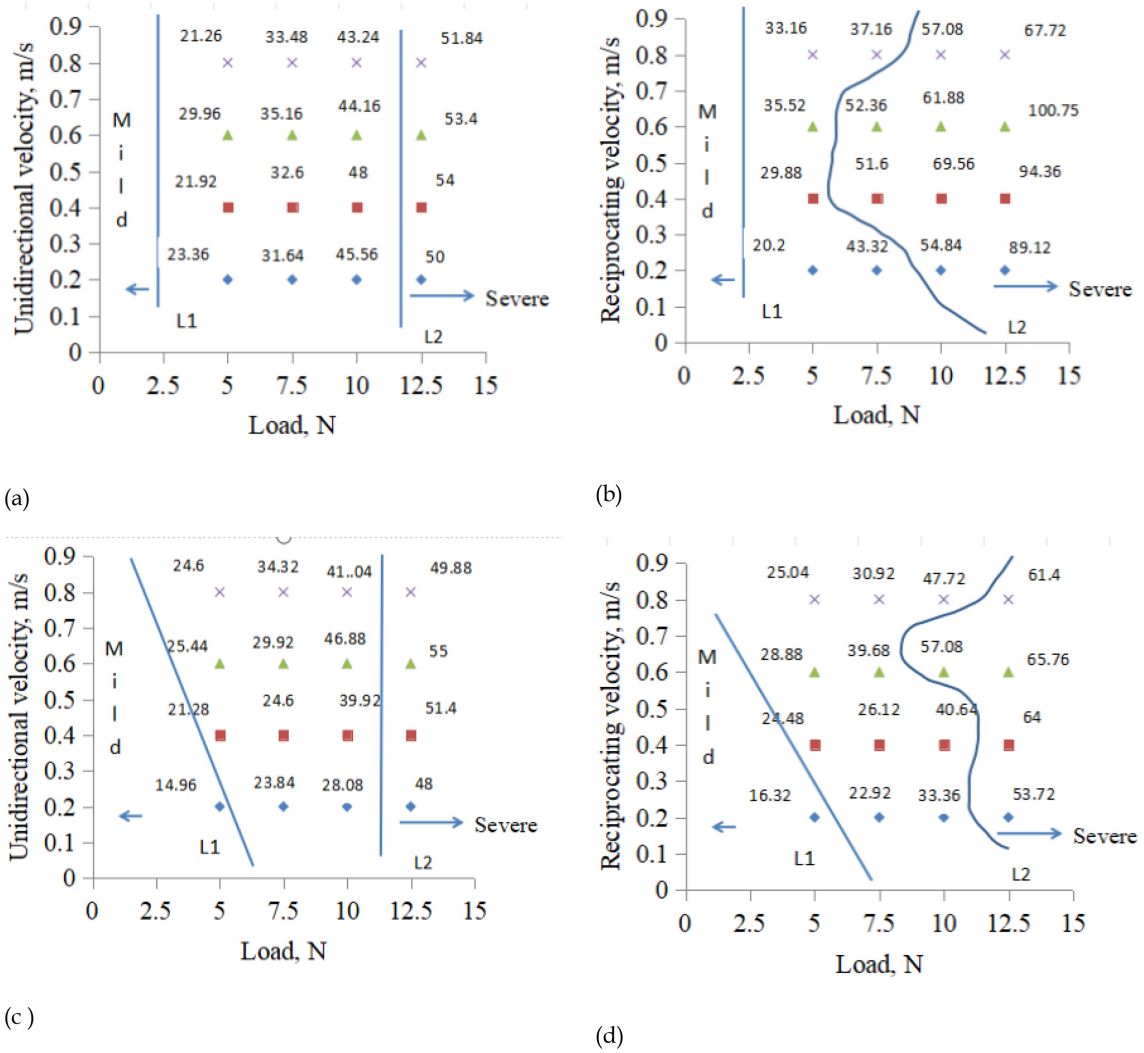

Figure 4. Abrasive wear mechanism maps for different loading and velocity conditions for a) A356 alloy USM b) A356 alloy in RSM c) A356+5wt.% SiCp composites in USM d) A356+5wt.%SiCp composites in RSM against 800grit for a sliding distance of 25m. Values multiplied by 10^{-5} indicate the wear rate. (Severe means higher wear rate at this particular experiment). Region below L1 indicates mild wear region.)

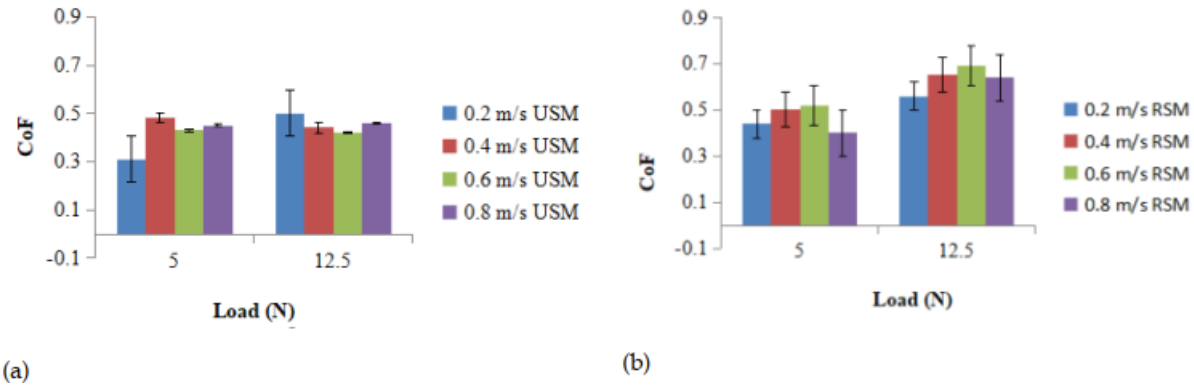

Figure 5. Varaition of CoF between tribopairs - slid for 25m against 800 grit SiC abrasive medium at loads 5N,12.5N for the velocity range 0.2-0.8 m/s in a) Unidirectional and b) Reciprocating contact for A356/5wt.% SiCp composite.

rate at this particular experiment, which is more than x10^{-5} g/m). Wear maps help to study and predict the wear characteristics of one material sliding against another at different sliding speeds and loads.

In figure 4 (a, b, c, d), below the line L1 indicates the mild wear regime and up to the lines L2 indicates the transition wear regime and above line L2 indicates the severe wear regimes. (In RSM and USM, the wear regimes are different for A356 alloy and A356/5wt.% SiCp composite. In our analysis severe abrasive wear is taken as above 50x10 $^{-5}$ gm./m. From abrasive wear map of A356 alloy, it is noted that severe wear starts when load reaches 12.5 N in USM. But in RSM, severe starts in between 5N and 7.5N for 0.4 and 0.6 m/s velocity conditions. For A356/5 wt.% composite, in USM, severe wear starts at almost 12.5 N. But in RSM it starts at 10N for 0.6 m/s. Transition from mild abrasive to severe abrasive wear starts in RSM for A356 at a lesser parametric combinations than in USM. It starts in between 5N and 7.5 N for velocities 0.4 and 0.6 m/s, but in USM it is 12.5 N for all velocity conditions.

Figure 5 depicts the variation of CoF between tribopairs - slid for 25 m against 800 grit SiC abrasive medium at loads 5N,12.5N for the velocity range 0.2-0.8 m/s in a) Unidirectional and b) Reciprocating contact for A356/5wt.% Si Cp composite. For A356 alloy and its composite, the general trend of CoF is increase with respect to load. It is attributed due to debris entrapment and surface fragmentation (R.K. Singh et al.). The composite consistently exhibited lower CoF values than the unreinforced alloy across all test conditions. At low loads, stable mechanically mixed layers reduced CoF, while at higher loads, increased fragmentation led to greater roughness and friction . For the A356 alloy, the CoF varied between 0.35 and 0.72, with higher values typically observed in USM at intermediate velocities. In comparison, the composite demonstrated a CoF range of 0.28 to 0.61, corresponding to an average reduction of approximately 20.7% relative to the base alloy. This reduction is attributed to the presence of hard SiCp particles, which minimize adhesive interactions at the sliding interface and contribute to improved load distribution. The composite also displayed more consistent frictional behaviour under increasing loads, indicating enhanced suitability for applications where frictional stability and wear resistance are critical.

For A356 alloy, the CoF is found to decrease with the entire velocity range tested in USM and RSM. The reduction at higher velocities is attributed to thermal softening and tribochemical reactions at the sliding interface, promoting tribolayer formation that acts as a solid lubricant (Ravikiran and Surappa, 1997)[17]. While for composites, CoF is found to increase with velocity in general. The lower CoF in USM compared to RSM under identical parametric conditions is due to the likelihood that deposits of plowed material in front of the slider will appear over a more extended timeframe than those in reciprocating contact (Blau and Walukas, 2000)[18].

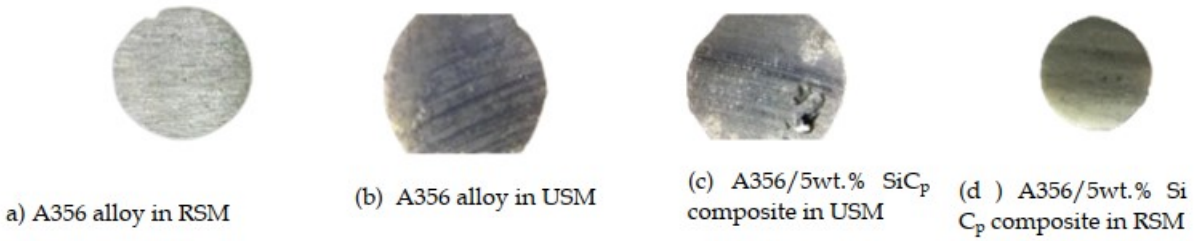

Figure 6. Stereo image of worn out surface of a) A356 alloy in RSM (b) A356 alloy in USM (c) A356+5wt.% SiC_p composite in RSM (d) A356+5wt.% SiC_p composite in RSM at 10 N, 0.6 m/s for a sliding distance of 25 m. skid against 800 grit abrasive medium.

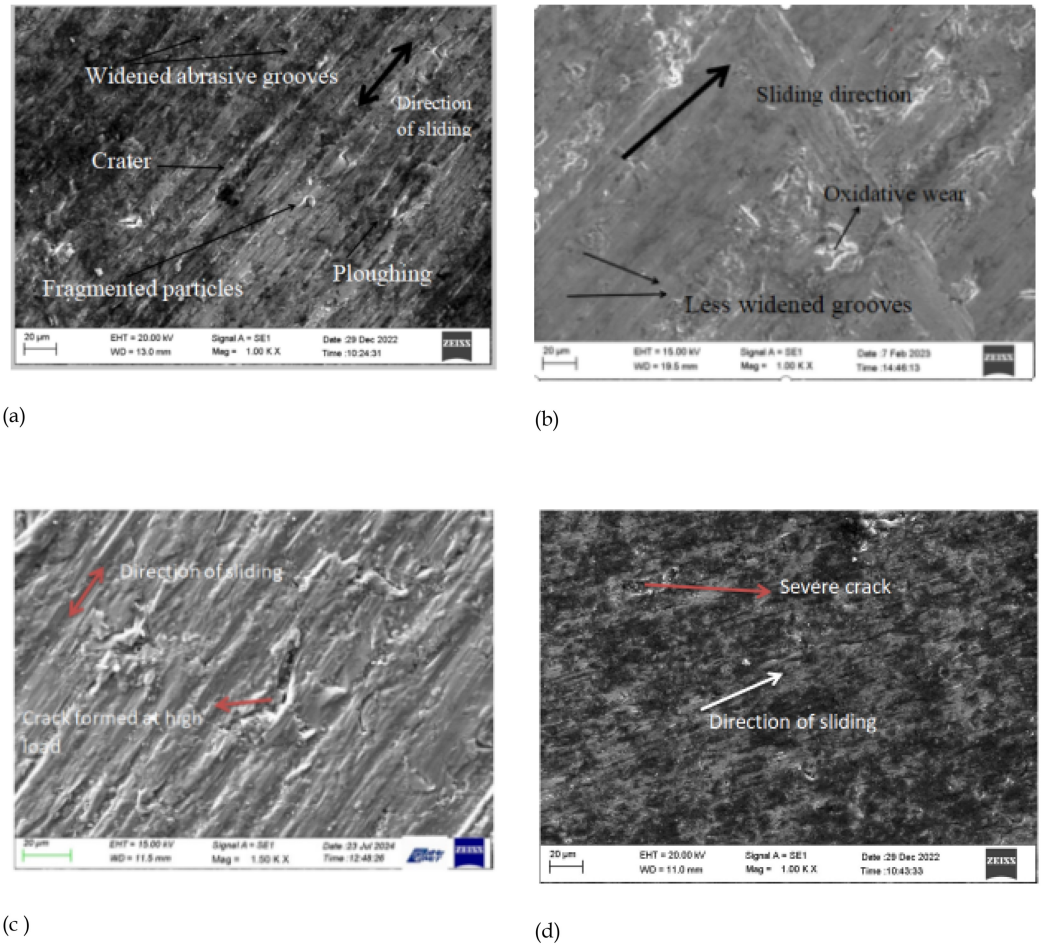

Figure 7. SEM images of worn out surface of (a) A356 alloy in RSM (b) A356 alloy in USM (c) A356/ 5 wt.% SiC_p composite in RSM and (d) A356/ 5 wt.% SiC_p composite in USM abraded against 18.3 microns SiC for a sliding distance of 25 m at 10 N, 0.6 m/s

3.3 Stereo microscopic analysis

Figure 6. depicts the stereo image of worn out surface of a) A356 alloy in RSM (b) A356 alloy in USM (c) A356/5wt.% SiCp composite in USM (d) A356/5wt.% SiC_p composite in RSM in sliding against 800 grit abrasive medium for 25 metre at 10N, 0.6 m/s. In USM, direction of sliding is along single direction, but in RSM it is in bidirection with widened and deepened grooves which indicates the severity of RSM than in USM under the same parametric conditions of abrasive wear applications. Entire surface wear out in RSM and not in USM. Abrasive groove width width and depth are more in RSM than in USM.

3.4 SEM /EDAX analysis of worn out surface of A356 alloy, A356/5wt.% SiC composite in unidirectional and reciprocating contacts (10 N, 0.6 m/s)

Figure 7. depicts the SEM images of worn out surface of (a) A356 alloy in RSM (b) A356 alloy in USM (c) A356/5 wt.% SiCp composite in RSM (d) A356/5 wt.% SiC composite in USM abraded against 800 grit SiC for a sliding distance of 25 metre at 10 N, 0.6 m/s.

SEM images of worn A356 alloy surfaces in RSM (Fig. 7a) show widened and depther grooves, fragmented particles, and craters due to ploughing, whereas USM (Fig. 7b) reveals shorter and less deepened grooves and signs of oxidative wear.

A356/5 wt.% composite in RSM (Fig. 7c) exhibits deeper grooves and crater formation, indicating transition wear, while USM (Fig.7d) shows shallow, narrower and deeper grooves typical of two-body abrasion. Groove widths decreases from alloy to composite and are significantly larger in RSM—2.781 µm in USM vs. 15.12 µm in RSM under 10 N, 0.6 m/s for the wornout surface of composite. RSM also shows more delamination wear due to mechanically mixed layer breakdown and SiC fragmentation, which increases wear rate [19]. Reinforcement particle escape can cause three-body abrasion, while Rigney [20] linked wear severity to hardness variation between tribopairs; composite shows more wear resistance attributed to its increased hardness due to SiC reinforcement bonding with matrix alloy at T6 heat treated conditon.

Figure 8. Depicts the EDAX analysis of SEM images of A356 Alloy in (a) RSM (b) USM and A356/5 wt.% composite in (c) RSM (d) USM respectively at 10 N, 0.6 m/s for a sliding distance of 25 metre. against 800 grit size

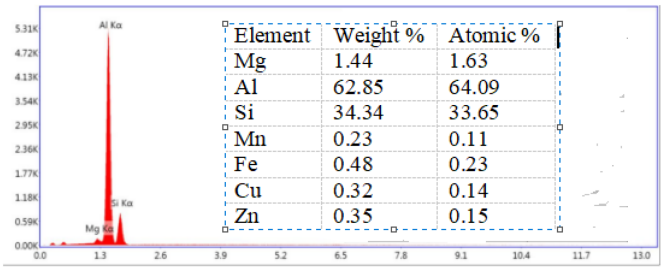

(a) RSM alloy

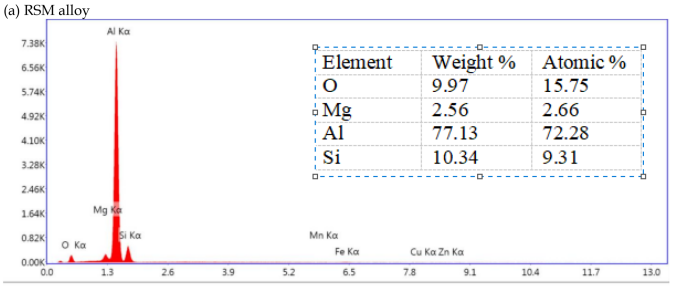

(b) USM alloy

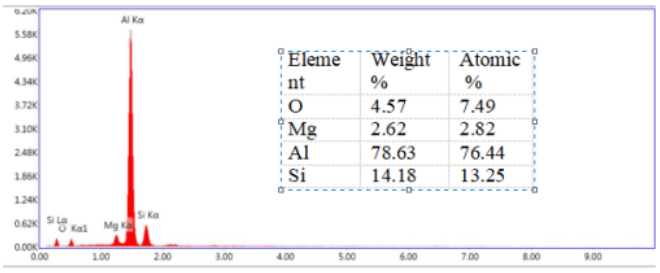

(c) RSM Composite

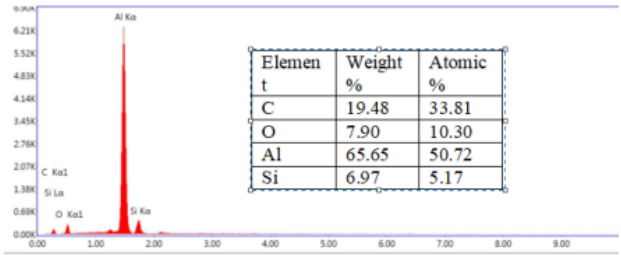

(d) USM Composite

Figure 8. EDAX analysis of A356 Alloy in (a) RSM (b) USM and A356/5 wt.% composite in (c) RSM (d) USM at 10 N, 0.6 m/s for a sliding distance of 25 metre. against 800 grit size SiC abrasive particles.

SiC abrasive particles. Figure 8 (a,b) illustrates the EDAX analyses of the A356 alloy under 10N, 0.6 m/s in USM and RSM condition reespectively. For alloys/composites, entire area of the worn out surface was selected for the analysis to minimise the error. In RSM (Fig. 8a), the alloy exhibits elemental compositions of Mg - 1.44 %, Al - 62.85 %, Si - 34.34 %, with minor traces of Mn, Fe, Cu, and Zn. In contrast, the USM condition (Fig. 8b) reveals the presence of O 9.97 %, Mg 2.56 %, Al 77.13 %, and Si 10.34 %. Presence of Silicon in all EDAX analysis represents the back transfer of silicon from abrasive medium during testing. Notably, oxygen is absent in RSM. But in USM, oxygen content is 9.97% ; indicating surface oxidation occurs predominantly during USM, particularly under 10 N load, 0.6 m/s sliding speed, and a 25 m distance against SiC (800 grit) abrasive. Tribo-oxidation in aluminium composites is governed by abrasion-induced film breakdown, flash-temperature-driven oxide formation, and cyclic regeneration of Al_2O_3.

Under high-velocity of sliding (10 N, 0.6 m/s), both A356 alloy and A356/5 wt.% SiC composite exhibited greater oxidative wear in USM compared to RSM. Oxygen content in USM reached 7.90%, against 4.57% in RSM—a 45.94% increase. This heightened oxide presence, as noted by Meher [21], correlates with increased oxide wear.

EDAX analysis of A356 + 5 wt.% SiCp composite under 10 N load and 0.6 m/s, over a 25 m slide against 800-grit SiC revealed, in RSM (Fig. 8c), Mg - 2.62%, Al - 78.63%, Si - 14.18%, and O - 4.57%. In contrast, USM (Fig.8d) showed O -7.90%, Al - 65.65%, and Si - 6.97%, indicating increased oxidation and reduced matrix elements under unidirectional sliding conditions. There are variations in elemental weight percentages for two distinct sliding modes—USM and RSM—applied to (a) A356 alloy and (b) A356/5 wt.% SiCp composite. For A356 alloy under RSM, the composition comprised O - 0%, Mg - 1.44%, Al- 62.85%, and Si - 34.34%, whereas USM revealed increased oxygen content (O- 9.97%), along with Mg - 2.56%, Al - 77.13%, and Si - 10.34%. The absence of oxygen in RSM and its significant presence in USM indicates enhanced oxidative wear under unidirectional sliding conditions.

In RSM, oxygen presence cannot seen which indicates zero oxidative abrasive wear in A356 alloy during RSM at 10N, 0.6 m/s. Less CoF in USM compared to RSM between tribo pairs is due to this oxide layer formation in USM, which is attributed due to the action of barrier by formation oxide layer in between tribopairs, which will reduce the direct contact between tribo pairs at this condition.

4. Conclusions

Wear rate in unidirectional and reciprocating mode are different even if the experiments are conducted at the same sliding conditions. Comparison studies shown that wear rate in reciprocating mode is higher than unidirectional mode.

1. A356/5 wt.% SiC composite prepared through stir casting route showed an enhancement of Brinell hardness values of about 12.19% -an enhanced abrasive wear resistance property.
2. In A356 alloy Severe wear starts when load reaches 12.5 N in USM. But in RSM, severe starts in between 5N and 7.5N for 0.4 and 0.6 m/s velocity conditions. For A356/5 wt.% composite, in USM, severe wear starts at almost 12.5 N. But in RSM it starts at 10N for 0.6 m/s
3. SEM images of worn A356 alloy surfaces in RSM shows widened and deeper grooves, fragmented particles, and craters due to ploughing, whereas USM reveals shorter

grooves and signs of oxidative wear. A356/5 wt.% composite in RSM exhibits large wider and deeper grooves and large crater formation (less compared to alloy), compared to USM shows less wider and deep grooves and less crater formation.

4. For A356 alloy under RSM, the composition comprised O - 0%, Mg - 1.44%, Al- 62.85%, and Si - 34.34%, whereas USM revealed increased oxygen content (O 9.97%), along with Mg - 2.56%, Al - 77.13%, and Si - 10.34%. The absence of oxygen in RSM and its significant presence in USM indicates enhanced oxidative wear under unidirectional sliding conditions.

Future scope: The future scope identified in this work is to characterize the subsurface study involved in the two abrasive sliding modes viz. reciprocating and unidirectional.

Acknowledgement

The authors are deeply acknowledging the fund received from the Centre for Engineering Research and Development (CERD), APJ Abdul Kalam Technological University, Government of Kerala, India

References

[1] R. L. Deuis, C Subramanian and J. M Yellup, Abrasive wear of aluminium composites-a review, Wear 201 (1996) 132-144 https://doi.org/10.1016/S0043-1648(96)07228-6

[2] X Y Li et al., Microstructural characterization of mechanically mixed layer and wear debris in sliding wear of an Al alloy and an Al based composite, Wear, Volume 245, Issues 1-2, 2000, Pages 148-161 https://doi.org/10.1016/S0043-1648(00)00475-0

[3] D. P. Mondal, S. Das, A.K. Jha & A.H. Yegneswaran, Abrasive wear of Al alloy-Al2O3 particle composite: a study on the combined effect of load and size of abrasive, Wear, Volume 223, Issues 1-2, 1998, Pages 131-138 https://doi.org/10.1016/S0043-1648(98)00278-6

[4] S Das, D P Mondal, S Sawla and S. Dixit, High Stress Abrasive Wear Mechanism of LM13-SiC Composite under Varying Experimental Conditions, Metallurgical and Materials Transactions A, Volume 33A, 2022, 3031-3044 https://doi.org/10.1007/s11661-002-0288-x

[5] D P Mondal, S Das, Tribology international, High stress abrasive wear behaviour of aluminium hard particle composites:Effect of experimental parameters, particle size and volumefraction, Tribology International, Volume 39, Issue 6, 2006, Pages 470-478 https://doi.org/10.1016/j.triboint.2005.03.003

[6] V.R. Rajeev, D.K. Dwivedi, S.C. Jain, Effect of load and reciprocating velocity on the transition from mild to severe wear behavior of Al-Si-SiCp composites in reciprocating conditions, Materials & Design, Volume 31, Issue10(2010), Pages 4951-4959 https://doi.org/10.1016/j.matdes.2010.05.010

[7] D. Odabas and S Su, A comparison of the reciprocating and continuous two body abrasive wear behavior of solution treated and age hardened 2014 Al alloy, Wear 208 (1997),25-35 https://doi.org/10.1016/S0043-1648(96)07378-4

[8] Paul G Panicker, N.Sasi, V.R.Rajeev, N.Asok Kumar. An integrated test bench device for testing of frictional behavior of materials, Official Journal of The Patent Office (India) Issue No.29/2019, date: 19/07/2019 Patent grant No. 414730, dated 16/12/2022.

[9] V. D. Gonçalves et al., A mechatronic system applied to wear particle analysis, Tribologia - Finnish Journal of Tribology, 4, vol 27/2008

[10] Premkumar John, Rajeev Vamadevan Rajam and Rajkumar Mattacaud Ramachandralal, "Dry wear behavior of A356-SiCp functionally graded composite in unidirectional and reciprocating contacts", Industrial Lubrication and Tribology, 73, 8,(2021), 1105-1112. https://doi.org/10.1108/ILT-04-2021-0139

[11] Y.Sahin, Wear behaviour of aluminium alloy and its composites reinforced by SiC particles using statistical analysis, Materials and Design, 24(2003), 95-103 https://doi.org/10.1016/S0261-3069(02)00143-7

[12] TPD Rajan et al., Fabrication and characterisation of Al-7Si-0.35 Mg/fly ash metal matrix composites processed by different stir casting routes, Composites Science and Technology, Volume 67, Issue 15-16, pages 3369-3377 https://doi.org/10.1016/j.compscitech.2007.03.028

[13] B. C. Pai, GeethaRamani, R. M. Pillai and K. G. Satyanarayana, Role of magnesium in cast aluminiurn alloy matrix composites, Journal of materials science, 30 (1995) 1903-1911 https://doi.org/10.1007/BF00353012

[14] GurpreetSingha and Neeraj Sharma, Study on the influence of T4 and T6 heat treatment on the wear behavior of coarse and fine WC particulate reinforced LM28 Aluminium cast composites, Composite-Part C, Open access 4 (2021) 100106 https://doi.org/10.1016/j.jcomc.2021.100106

[15] J. Hashim, L. Looney and M.S.J. Hashmi, Metal matrix composites: production by the stir casting method, Journal of Materials Processing Technology, 92-93 (1999) 1-7 https://doi.org/10.1016/S0924-0136(99)00118-1

[16] A, T. Alpas and J.D, Embury, Prac. Conf. Wear of Materials. ASME, New York, 1991, p, 159

[17] A Ravikiran, M.K Surappa, "Effect of sliding speed

on wear behaviour of A356 Al-30 wt.% SiCp MMC", Wear, Volume 206, Issues 1-2 (1997), Pages 33-38 https://doi.org/10.1016/S0043-1648(96)07341-3

[18] Blau, P.J. and Walukas, M. , "Sliding friction and wear of magnesium alloy AZ91D produced by two different methods", Tribology International, Vol. 33 No. 8 (2000), pp. 573-579 https://doi.org/10.1016/S0301-679X(00)00108-0

[19] Gurpreet Singh et al., Development and tribological investigation of B4C reinforced AA5082 Aluminum alloy cast composites for automotive applications, 2024 Eng. Res. Express 6 015073 https://doi.org/10.1088/2631-8695/ad1f10

[20] Rigney D. A., Comments on the sliding wear of metals, Tribol Int., 1997;30:361-367. https://doi.org/10.1016/S0301-679X(96)00065-5

[21] Arabinda Meher et al., Study on effect of TiB2 reinforcement on the microstructural and mechanical properties of magnesium RZ5 alloy based metal matrix composites, Journal of Magnesium and Alloys, Volume 8, Issue 3, 2020, Pages 780-792 https://doi.org/10.1016/j.jma.2020.04.003